

# Two-phonon $\gamma$ -vibrational states in rotating triaxial odd- $A$ nuclei

Masayuki Matsuzaki\*

*Department of Physics, Fukuoka University of Education,  
Munakata, Fukuoka 811-4192, Japan*

(Dated: January 11, 2013)

## Abstract

Distribution of the two phonon  $\gamma$  vibrational collectivity in the rotating triaxial odd- $A$  nucleus,  $^{103}\text{Nb}$ , that is one of the three nuclides for which experimental data were reported recently, is calculated in the framework of the particle vibration coupling model based on the cranked shell model plus random phase approximation. This framework was previously utilized for analyses of the zero and one phonon bands in other mass region and is applied to the two phonon band for the first time. In the present calculation, three sequences of two phonon bands share collectivity almost equally at finite rotation whereas the  $K = \Omega + 4$  state is the purest at zero rotation.

PACS numbers: 21.10.Re, 21.60.Jz, 27.60.+j

---

\*matsuza@fukuoka-edu.ac.jp

## I. INTRODUCTION

One of the properties most specific to the finite quantum many body system, the atomic nucleus, is to exhibit both single particle and collective modes of excitation in similar energy scale.

Thanks to recent progress in computer power, exact diagonalization of given effective interaction in a huge model space is becoming available for up to medium mass nuclei including those far from stability. But in order to extract physical picture of their dynamics from huge numerical information, it is necessary to have recourse to the concept of collectivity. Among the various kinds of collective modes of excitation, one of those that have been well studied and known to exist prevailingly in the nuclear chart is the  $\gamma$  vibration. Vibrational excitations in many fermion systems, in other terms, phonons, are made up by coherent superposition of particle-hole or two quasiparticle excitations. Thus, on the one hand, multiple excitations are expected if they are really collective. On the other hand, their excitation spectra, in particular their anharmonicity reflect underlying nuclear structure.

In the nuclear chart, collective vibrations in the rare earth nuclei with the mass  $A = 160 - 170$  are the best studied. The first experimental information about the two phonon  $\gamma$  vibration, denoted by the  $2\gamma$  hereafter, in  $^{168}\text{Er}$  was reported by Davidson et al. [1] based on a high resolution  $\gamma$  ray study following neutron capture. The first theoretical analysis was done by Warner et al. [2] in terms of the interacting boson model with  $s$  and  $d$  bosons but it was critically assessed by Bohr and Mottelson [3]. They argued within the general framework applicable to deformed nuclei with rotational spectra [4]. Dumitrescu and Hamamoto [5] elucidated this problem by means of a macroscopic and microscopic analysis. On the contrary, Soloviev and Shirikova [6] argued that collective two phonon excitations do not exist because of the strong Pauli principle among nucleons that constitute vibrational excitations based on the quasiparticle phonon model. Matsuo [7] and Matsuo and Matsuyanagi [8] applied the selfconsistent collective coordinate method that provides quantized collective Hamiltonian starting from the microscopic random phase approximation (RPA) and obtained the result that the  $K = 4$   $2\gamma$  state in the triaxially deformed potential exists at the energy about 2.7 times that of the  $1\gamma$  state. Pipenbring and Jammari [9] also obtained a similar result by means of the multiphonon method based on the Tamm-Dancoff approximation. The description in terms of the interacting boson model was improved by Yoshinaga et al. [10]

by introducing the  $g$  boson. The definite experimental evidence, the absolute  $B(E2)$  value between the  $K = 4$   $2\gamma$  candidate and the  $1\gamma$ , that proves that the  $K = 4$  state is really the  $2\gamma$  was given by means of  $\gamma$  ray induced Doppler broadening following neutron capture by Börner et al. [11] and using Coulomb excitation by Oshima et al. [12] and Härtlein et al. [13].

The  $2\gamma$  states of very similar character were predicted [8, 14] and observed in nearby nuclides,  $^{166}\text{Er}$  using Coulomb excitation by Fahlander et al. [15] and using a  $(n, n'\gamma)$  reaction by Garrett et al. [16], and  $^{164}\text{Dy}$  using thermal neutron capture by Corminboeuf et al. [17]. In particular, the  $K = 0$   $2\gamma$  state was also observed in  $^{166}\text{Er}$  [16]. Sun et al. [18] studied the  $2\gamma$  bands in  $^{166,168}\text{Er}$  in terms of the triaxial projected shell model. This model gives the  $K = 4$   $2\gamma$  states in a kinematical manner similar to Davydov-Filippov's asymmetric rotor model [19]. In other mass regions, harmonic  $2\gamma$  states were observed in  $^{232}\text{Th}$  by Korten et al. [20, 21] using Coulomb excitation and  $^{106,104}\text{Mo}$  by Guessous et al. [22, 23] using a spontaneous fission. The latter was discussed from a viewpoint of the  $X(5)$  symmetry [24]. These very limited number of observations indicate that it depends strongly on the underlying single particle level structure whether the  $2\gamma$  states exist or not. This fact suggests that microscopic description of the collective vibrational excitations is mandatory.

In odd- $A$  nuclei, some numerical prediction for rare earth nuclides were made by Durand and Piepenbring [25] in terms of the multiphonon method prior to experimental observation. The first experimental observation was made ten years later in  $^{105}\text{Mo}$  by Ding et al. [26] using a spontaneous fission. In these fission fragments,  $^{104-106}\text{Mo}$ , rotational band members built on the  $2\gamma$  states were also populated. Soon after this, similar rotational bands were observed also in  $^{103}\text{Nb}$  by Wang et al. [27] and  $^{107}\text{Tc}$  by Long et al. [28]. These nuclei exhibit anharmonicity  $E_{2\gamma}/E_{1\gamma} < 2$  in  $^{105}\text{Mo}$  and  $^{103}\text{Nb}$ , while  $\gtrsim 2$  in  $^{107}\text{Tc}$ , where level energies are measured from the corresponding zero phonon states. These are the  $2\gamma$  states observed so far. The first theoretical calculation to the observed  $2\gamma$  band in the odd- $A$  nucleus,  $^{103}\text{Nb}$ , was done by Sheikh et al. [29] in terms of the triaxial projected shell model. It was discussed there that the observed anharmonicity is difficult to be reproduced with the triaxial parameter that gives a good description of the  $1\gamma$  band.

In the present paper, we take a complementary approach to the  $2\gamma$  band in  $^{103}\text{Nb}$ ; the particle vibration coupling (PVC) calculation based on the RPA phonons constructed in the rotating frame allowing possible static triaxial deformation.

## II. THE MODEL

In the model adopted in this study, elementary modes are quasiparticles and  $\gamma$  vibrational RPA phonons excited on top of common vacuum as in traditional calculations, however, the vacuum is the yrast configuration of an even-even nucleus rotating with a frequency  $\omega_{\text{rot}}$ . This vacuum configuration can be either zero quasiparticle, two quasiparticle and so on, seen from the non-rotating ground state. Excitations are labeled by the signature quantum number  $r = \exp(-i\pi\alpha)$ ,  $I = \alpha + \text{even}$ , appropriate for rotating reflection-symmetric objects. Two kinds of  $\gamma$  vibrational excitations exist, denoted by  $X_{\gamma(\pm)}^\dagger$  with  $r = \pm 1$ , respectively. The phonon space is limited to zero, one and two phonon states. The vacuum mean field is rotating and static triaxial deformation is also possible; this means that the  $\Omega$ -mixing in quasiparticles and the  $K$ -mixing in RPA phonons are naturally taken into account. Here  $\Omega$  is the projection of the single particle angular momentum to the third axis.

The formulation is summarized as follows. We begin with a one-body Hamiltonian in the rotating frame,

$$h' = h - \omega_{\text{rot}} J_x, \quad (1)$$

$$h = h_{\text{Nil}} - \Delta_\tau (P_\tau^\dagger + P_\tau) - \lambda_\tau N_\tau, \quad (2)$$

$$h_{\text{Nil}} = \frac{\mathbf{p}^2}{2M} + \frac{1}{2} M (\omega_x^2 x^2 + \omega_y^2 y^2 + \omega_z^2 z^2) + v_{ls} \mathbf{l} \cdot \mathbf{s} + v_{ll} (\mathbf{l}^2 - \langle \mathbf{l}^2 \rangle_{N_{\text{osc}}}). \quad (3)$$

In Eq. (2),  $P_\tau$  is the pair annihilation operator,  $\tau = 1$  and  $2$  denote neutron and proton, respectively, and the chemical potentials  $\lambda_\tau$  are determined so as to give the correct average particle numbers  $\langle N_\tau \rangle$ . The oscillator frequencies in Eq. (3) are related to the quadrupole deformation parameters  $\epsilon_2$  and  $\gamma$  in the usual way. They, along with the pairing gaps  $\Delta_\tau$ , are determined from experimental information. The orbital angular momentum  $\mathbf{l}$  in Eq. (3) is defined in the singly stretched coordinates  $x'_k = \sqrt{\frac{\omega_k}{\omega_0}} x_k$  and the corresponding momenta, with  $k = 1, 2$  and  $3$  denoting  $x, y$  and  $z$ , respectively. We apply the RPA to the residual pairing plus doubly stretched quadrupole-quadrupole ( $Q'' \cdot Q''$ ) interaction between quasiparticles. It is given by

$$H_{\text{int}} = - \sum_{\tau=1,2} G_\tau \tilde{P}_\tau^\dagger \tilde{P}_\tau - \frac{1}{2} \sum_{K=0,1,2} \kappa_K^{(+)} Q_K''{}^{(+)\dagger} Q_K''{}^{(+)} - \frac{1}{2} \sum_{K=1,2} \kappa_K^{(-)} Q_K''{}^{(-)\dagger} Q_K''{}^{(-)}, \quad (4)$$

where the doubly stretched quadrupole operators are defined by

$$Q_K'' = Q_K(x_k \rightarrow x'_k = \frac{\omega_k}{\omega_0} x_k), \quad (5)$$

and those with good signature are

$$Q_K^{(\pm)} = \frac{1}{\sqrt{2(1 + \delta_{K0})}} (Q_K \pm Q_{-K}), \quad (6)$$

and  $\tilde{P}_\tau$  is defined by subtracting the vacuum expectation value from  $P_\tau$ . Among RPA modes determined by the equation of motion,

$$[h' + H_{\text{int}}, X_n^\dagger]_{\text{RPA}} = \omega_n X_n^\dagger, \quad (7)$$

we choose the  $\gamma$  vibrational phonons,  $n = \gamma(\pm)$ , which have outstandingly large  $K = 2$  transition amplitudes

$$|T_K^{(\pm)}| = \left| \left\langle \left[ Q_K^{(\pm)}, X_{\gamma(\pm)}^\dagger \right] \right\rangle \right|. \quad (8)$$

The particle vibration coupling Hamiltonian takes the form

$$\begin{aligned} H_{\text{couple}}(\gamma) &= \sum_{\mu\nu} \Lambda_{\gamma(+)}(\mu\nu) \left( X_{\gamma(+)}^\dagger a_\mu^\dagger a_\nu + X_{\gamma(+)} a_\nu^\dagger a_\mu \right) \\ &\quad + \sum_{\bar{\mu}\bar{\nu}} \Lambda_{\gamma(+)}(\bar{\mu}\bar{\nu}) \left( X_{\gamma(+)}^\dagger a_{\bar{\mu}}^\dagger a_{\bar{\nu}} + X_{\gamma(+)} a_{\bar{\nu}}^\dagger a_{\bar{\mu}} \right) \\ &\quad + \sum_{\mu\bar{\nu}} \Lambda_{\gamma(-)}(\mu\bar{\nu}) \left( X_{\gamma(-)}^\dagger a_\mu^\dagger a_{\bar{\nu}} + X_{\gamma(-)} a_{\bar{\nu}}^\dagger a_\mu \right) \\ &\quad + \sum_{\bar{\mu}\nu} \Lambda_{\gamma(-)}(\bar{\mu}\nu) \left( X_{\gamma(-)}^\dagger a_{\bar{\mu}}^\dagger a_\nu + X_{\gamma(-)} a_\nu^\dagger a_{\bar{\mu}} \right), \end{aligned} \quad (9)$$

where  $\mu$  and  $\bar{\mu}$  denote quasiparticles with  $r = -i$  and  $+i$ , respectively. The coupling vertices are given by

$$\begin{aligned} \Lambda_{\gamma(+)}(\mu\nu) &= - \sum_{K=0,1,2} \kappa_K^{(+)} T_K''^{(+)} Q_K''^{(+)}(\mu\nu), \\ \Lambda_{\gamma(+)}(\bar{\mu}\bar{\nu}) &= - \sum_{K=0,1,2} \kappa_K^{(+)} T_K''^{(+)} Q_K''^{(+)}(\bar{\mu}\bar{\nu}), \\ \Lambda_{\gamma(-)}(\mu\bar{\nu}) &= - \sum_{K=1,2} \kappa_K^{(-)} T_K''^{(-)} Q_K''^{(-)}(\mu\bar{\nu}), \\ \Lambda_{\gamma(-)}(\bar{\mu}\nu) &= - \sum_{K=1,2} \kappa_K^{(-)} T_K''^{(-)} Q_K''^{(-)}(\bar{\mu}\nu), \end{aligned} \quad (10)$$

where  $Q_K''^{(\pm)}(\alpha\beta)$  denotes quasiparticle scattering matrix elements that do not contribute to

RPA phonons. Eigenstates of the Hamiltonian thus specified at each  $\omega_{\text{rot}}$  take the form

$$\begin{aligned}
 |\chi_j\rangle = & \sum_{\mu} \psi_j^{(1)}(\mu) a_{\mu}^{\dagger} |\phi\rangle \\
 & + \sum_{\mu} \psi_j^{(3)}(\mu\gamma) a_{\mu}^{\dagger} X_{\gamma}^{\dagger} |\phi\rangle + \sum_{\bar{\mu}} \psi_j^{(3)}(\bar{\mu}\bar{\gamma}) a_{\bar{\mu}}^{\dagger} X_{\bar{\gamma}}^{\dagger} |\phi\rangle \\
 & + \sum_{\mu} \psi_j^{(5)}(\mu\gamma\gamma) \frac{1}{\sqrt{2}} a_{\mu}^{\dagger} X_{\gamma}^{\dagger} X_{\gamma}^{\dagger} |\phi\rangle + \sum_{\mu} \psi_j^{(5)}(\mu\bar{\gamma}\bar{\gamma}) \frac{1}{\sqrt{2}} a_{\mu}^{\dagger} X_{\bar{\gamma}}^{\dagger} X_{\bar{\gamma}}^{\dagger} |\phi\rangle \\
 & + \sum_{\bar{\mu}} \psi_j^{(5)}(\bar{\mu}\gamma\bar{\gamma}) a_{\bar{\mu}}^{\dagger} X_{\gamma}^{\dagger} X_{\bar{\gamma}}^{\dagger} |\phi\rangle,
 \end{aligned} \quad (11)$$

for the  $r = -i$  sector,

where  $\gamma$  and  $\bar{\gamma}$  abbreviate  $\gamma(+)$  and  $\gamma(-)$ , respectively, and  $|\phi\rangle$  is the rotating vacuum configuration. Those for the  $r = +i$  sector take a form similar to above, except that the suffices  $\mu$  are to be replaced by  $\bar{\mu}$ .

This model was first developed for studying the signature dependence of the level energies and  $E2$ ,  $M1$  transition rates in one quasiparticle (zero phonon) bands [30, 31], and then applied to study the  $E2$  intensity relation [4, 32] in the  $1\gamma$  rotational bands [33]. The present study is the first application to the  $2\gamma$  states in rotating odd- $A$  nuclei. By construction of the model space, this model is applicable up to the energy region  $\lesssim E_{1\text{qp}} + 2\Delta$ ; otherwise non-collective 3qp states dominate over the collective states.

### III. RESULTS AND DISCUSSIONS

Three new rotational bands that feed the  $\pi[422\ 5/2^+]$  ground band of  $^{103}_{41}\text{Nb}_{62}$  were observed by a very recent  $\gamma$  ray study of spontaneous fission fragments from  $^{252}\text{Cf}$  [27]. Among them, the one that is built on the  $9/2^+$  bandhead was assigned to the  $K = \Omega + 2$  sequence of the  $1\gamma$  bands. One of the others that is built on the  $13/2^+$  bandhead was assigned to the  $K = \Omega + 4$  sequence of the  $2\gamma$  bands. This is the second observation of the  $2\gamma$  band in odd- $A$  nuclei, and to which the first theoretical calculation [29] was reported. In the present cranked shell model calculation, diagonalization is performed in the five major shells,  $N_{\text{osc}} = 2 - 6$  for the neutron and  $1 - 5$  for the proton with the Nilsson parameters  $v_{ls}$  and  $v_{ll}$  taken from Ref. [34]. The three mean field parameters, which are assumed to be  $\omega_{\text{rot}}$  independent for simplicity, the pairing gaps  $\Delta_n = 1.05$  MeV,  $\Delta_p = 0.85$  MeV and the deformation  $\epsilon_2 = 0.31$  are adopted from the experimental analyses [22, 27]. The triaxiality  $\gamma$  is chosen so as to

reproduce the measured signature splitting of the ground band in the PVC calculation. The chosen value,  $\gamma = -7^\circ$ , gives overall reproduction of the signature splitting in the rotating frame aside from near the bandhead as shown in Fig. 1(a). Note here that it was reported that the signature splitting can be reproduced without invoking  $\gamma$  deformation in the ancestral model [35] of the triaxial projected shell model. This suggests that the appropriate value of the  $\gamma$  deformation is model dependent as noticed in Ref. [36] and discussed below.

The strengths of the residual doubly stretched quadrupole interaction are determined as follows; in the reference configuration with  $\omega_{\text{rot}} = 0$  and  $\gamma = 0$  in which  $K$  is a good quantum number,  $\kappa_2^{(+)} = \kappa_2^{(-)}$  is determined to reproduce within the RPA the observed  $\gamma$  vibrational energy in the adjacent  ${}^{104}\text{Mo}$ , 0.812 MeV. If fully collective  $\beta$  vibration exists,  $\kappa_0^{(+)}$  can be determined to reproduce its energy but since the collective character of the observed  $0_2^+$  is not clear,  $\kappa_0^{(+)}$  is set equal to  $\kappa_2^{(\pm)}$ . And  $\kappa_1^{(+)} = \kappa_1^{(-)}$  is determined so as to make the energy of the Nambu-Goldstone mode zero. Those of the residual pairing interaction are determined to reproduce the adopted pairing gaps. Then the RPA calculation is performed with  $\gamma = -7^\circ$ . The obtained  $\omega_{\text{rot}}$  dependence and signature splitting [4, 37] of the excitation energy of  $\gamma$  vibration is weak as shown in Fig. 1(b).

Using these quantities,  $H_{\text{couple}}(\gamma)$  is diagonalized in the space of dimension 15 (number of quasiparticle states with  $N_{\text{osc}} = 4$ )  $\times$  6 (1qp,  $1\text{qp} \otimes \gamma(+)$ ,  $\overline{1\text{qp}} \otimes \gamma(-)$ ,  $1\text{qp} \otimes \gamma(+)$   $\otimes \gamma(+)$ ,  $1\text{qp} \otimes \gamma(-)$   $\otimes \gamma(-)$ ,  $\overline{1\text{qp}} \otimes \gamma(+)$   $\otimes \gamma(-)$ , with bar denoting the opposite signature) for each signature sector. Distribution of the strength (probability in the wave function) of the  $\pi[422\,5/2^+] \otimes \gamma$  vibration(s) that shows the collectiveness of each eigenstate directly is presented in Fig. 2 for the case of the favored signature  $r = -i$ . The result for the unfavored  $r = +i$  is similar.

In the favored ( $r = -i$ ) sector, two dominantly  $1\gamma$  eigenstates are obtained as a result of the interaction between the  $f \otimes \gamma(+)$  and the  $u \otimes \gamma(-)$  basis states, hereafter  $f$  and  $u$  denote the favored and unfavored 1qp states originating from the  $\pi[422\,5/2^+]$ , respectively. There is no general rule of the correspondence between these two bands in the signature scheme and the  $K = \Omega \pm 2$  bands in the  $K$  scheme. However, since states with the lower  $K$  have lower intrinsic energies than those with higher  $K$  and the same  $I$ , the obtained lower band can be identified with the  $K = \Omega - 2$  band. Actually, in the previous analysis of the  $E2$  intensity relation [33], correspondence between the observed and the calculated states was established in this manner. The present result indicates that collectivity does not fragment

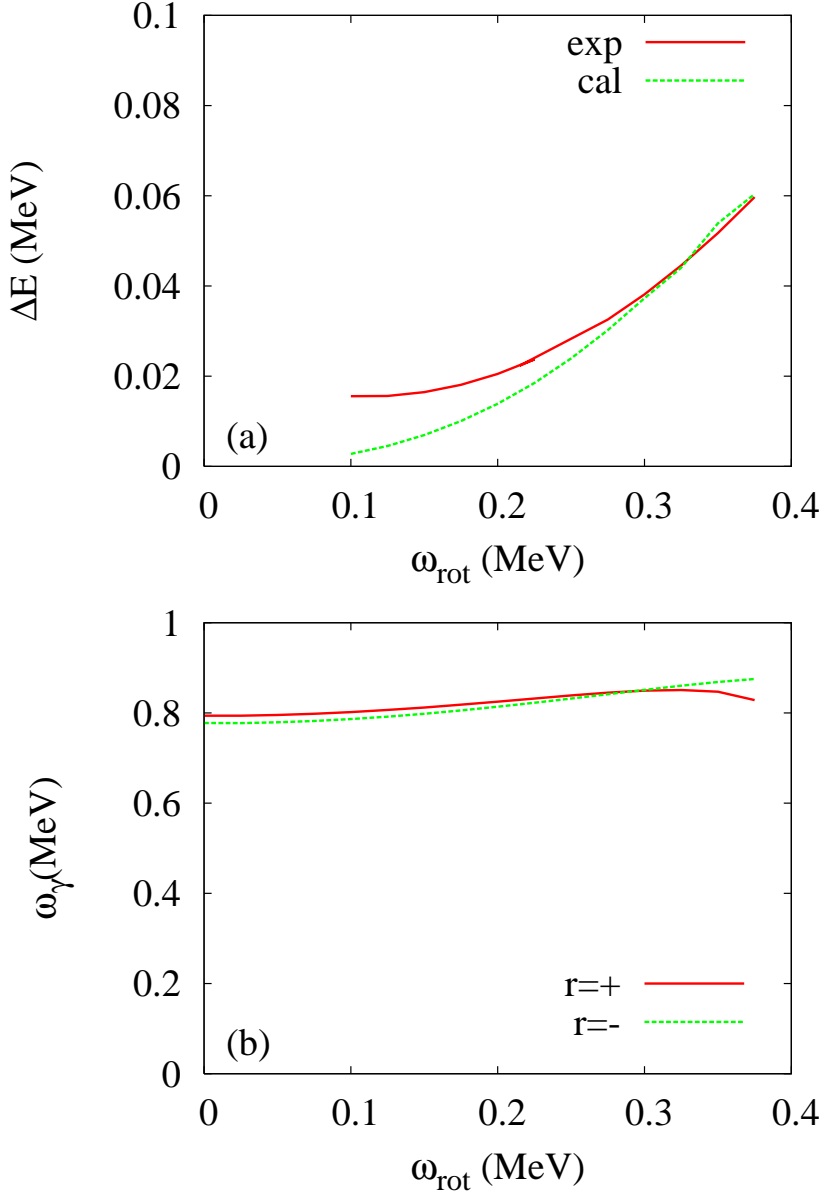


FIG. 1: (Color online) (a) Experimental and calculated signature splitting in the  $\pi[422\ 5/2^+]$  one quasiparticle band as functions of the rotation frequency. Theoretical curve is the result of the particle vibration coupling rather than the cranked shell model alone. The latter (not shown) is larger than the former. (b) Excitation energies of the two types of  $\gamma$  vibrational RPA phonons as functions of the rotation frequency.

much and two bands are almost parallel as in the  $^{165}\text{Ho}$  case [33]. But the higher band is slightly more collective and purer. This is consistent with the observation at  $\omega_{\text{rot}} = 0$  that states with lower  $K$  are affected more by interaction with other states [25, 38]. Actually only the  $K = \Omega + 2$  sequence was observed in many cases.

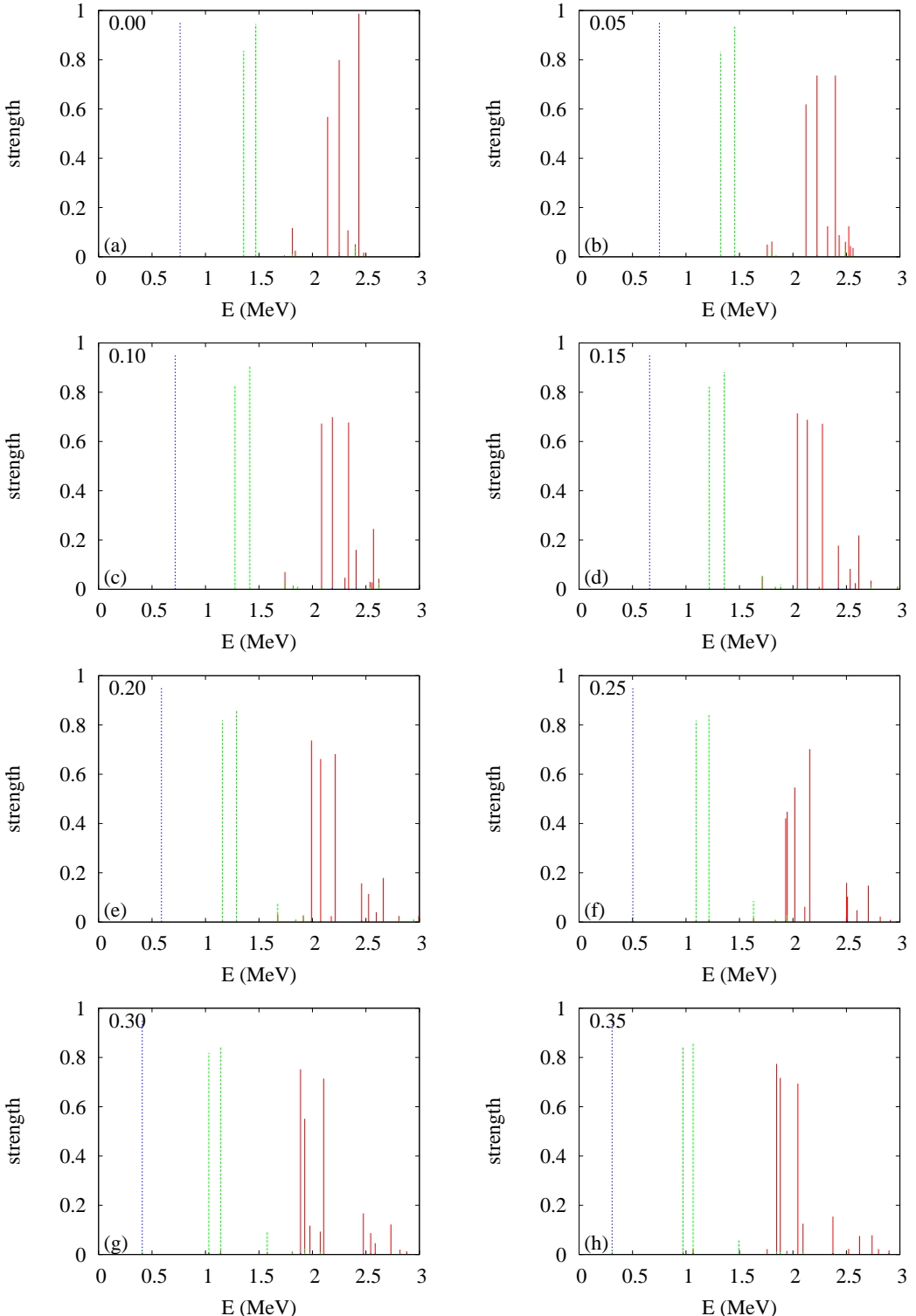


FIG. 2: (Color online) Distribution of the strength (probability in the wave function) of the 1qp,  $1qp \otimes \gamma$  and  $1qp \otimes \gamma \otimes \gamma$  components in the favored signature ( $r = -i$ ),  $|\psi^{(1)}(\mu)|^2$  (blue dotted),  $|\psi^{(3)}(\mu\gamma)|^2 + |\psi^{(3)}(\bar{\mu}\bar{\gamma})|^2$  (green dashed) and  $|\psi^{(5)}(\mu\gamma\gamma)|^2 + |\psi^{(5)}(\mu\bar{\gamma}\bar{\gamma})|^2 + |\psi^{(5)}(\bar{\mu}\bar{\gamma}\bar{\gamma})|^2$  (red solid), respectively, at various rotation frequencies,  $\omega_{\text{rot}} = 0 - 0.35$  MeV. Here 1qp ( $\mu$ ) means the one quasiparticle states originating from the  $\pi[422\ 5/2^+]$  at  $\omega_{\text{rot}} = 0$ .

Fragmentation of the  $2\gamma$  components is expected to depend sensitively on how other quasiparticle states distribute. In the present calculation, the  $2\gamma$  strength concentrates mainly on three eigenstates that locate at  $\lesssim E_{1\text{qp}} + 2\Delta_p$ . They are obtained as a result of the interaction among the  $f \otimes \gamma(+)\otimes \gamma(+)$ , the  $f \otimes \gamma(-)\otimes \gamma(-)$  and the  $u \otimes \gamma(+)\otimes \gamma(-)$  basis states. With the same rule as for the  $1\gamma$  case, they can be identified with  $K = |\Omega - 4|$ ,  $\Omega$  and  $\Omega + 4$  from the lower. At  $\omega_{\text{rot}} = 0$  the higher  $K$  states are the more collective as expected. But small rotation immediately mixes their collectivity. Then three collective bands run keeping almost the same collectivity.

In order to see how these collective states interact with other non-collective states, all the eigenstates of  $H_{\text{couple}}(\gamma)$  that locate lower than 3 MeV are shown in Fig. 3(a). At  $\omega_{\text{rot}} = 0$ , there are 2nd – 4th  $N_{\text{osc}} = 4$  1qp states between the  $1\gamma$ s and  $2\gamma$ s. These are expected to correspond to some of the levels that were known to be populated by the  $^{103}\text{Zr}$   $\beta$  decay but spin and parity have not been assigned [39]. One of them interacts with the  $2\gamma$ s depending on  $\omega_{\text{rot}}$ . Aside from this, the  $2\gamma$ s keep their collective characters as shown in Fig. 2.

Next the obtained collective states are compared with observed ones in Fig. 3(b). This figure shows that the 1qp and the  $1\gamma$  ( $K = \Omega + 2$ ) are reproduced almost perfectly. On the other hand, the calculated  $2\gamma$ s obviously locate higher than the observed one. The most probable reason of this is ignoring higher lying states, that is, their effect to push down the  $2\gamma$  states. Although one may be afraid that inclusion of more states would lead to fragmentation of collectivity, we expect this not to occur since the number of nearby states is still small.

Here we discuss the adopted triaxial deformation  $\gamma$  in Ref. [29] and the present calculation. It has two physical aspects, its sign and its absolute value. The former is originally the notion in the rotating mean field model. Although the projection model in its original framework does not distinguish the sign of  $\gamma$  to our knowledge, Ref. [36] proposed a method to find the main rotation axis. This made it possible to relate the result of the projection calculation to the sign of  $\gamma$ . In Ref. [29], the adopted  $\epsilon = 0.3$  and  $\epsilon' = 0.16$  correspond to  $\gamma = \pm 28^\circ$ . Although its sign is not described, odd- $A$  nuclei with an  $\Omega = 5/2$  odd nucleon show  $\gamma < 0$  rotation due to its shape driving effect in addition to the approximately irrotational property of the even-even core in general. Then we regard the sign is consistent with ours. As for the latter, its absolute value, the origin of the difference is that of the generating mechanism of the  $\gamma$  band itself as pointed out in Ref. [18]. It is constructed as

a vibrational phonon excitation built on top of the yrast configuration in our model. In contrast, in the projection model, it is generated as a rotational excitation in the sense of the asymmetric rotor. Consequently appropriate  $\gamma$  deformation is not necessarily the same. The latter calls for a larger  $|\gamma|$ ; for example,  $|\gamma| = 25^\circ$  was adopted for  $^{168}\text{Er}$  [18], which is regarded as a typical axially symmetric nucleus [4]. Note here that large fluctuations in the  $\gamma$  direction were shown for nuclei of that class, for example, in Ref. [40]. These results indicate that the model dependence of the adopted value of  $\gamma$  deformation is not unphysical. It is an interesting subject to look into more this longstanding problem of how these two, vibrational/rotational, descriptions are related, but it is beyond the scope of the present paper.

Last but not least, we mention another type of collective motion for which two phonon excitation was observed, the wobbling motion predicted by Bohr and Mottelson [4], Janssen and Mikhailov [41] and Marshalek [42], and first observed by Ødegård et al. [43]. This is a small amplitude fluctuation of the rotation axis of triaxially deformed nuclei and has the same quantum number,  $r = -1$ , as the odd spin members of the  $\gamma$  vibrational bands. Two phonon wobbling bands were observed in  $^{163}\text{Lu}$  by Jensen et al. [44] and  $^{165}\text{Lu}$  by Schönwaßer et al. [45]. Their excitation energies in the rotating frame exhibit anharmonicity such that the two phonon states locate lower than the twice the energies of the one phonon states. The present author and Ohtsubo [46] argued that this anharmonicity indicates the softening of the collective potential surface, that is, the precursor of the second order phase transition from the principal axis rotation to the tilted axis rotation. This is completely parallel with the situation that the softening of the  $\gamma$  vibration is the precursor of the second order phase transition from the axial symmetric deformation to static triaxial deformation. The new vacuum after the phase transition can accommodate anharmonic vibration either  $E_{2\text{-phonon}}/E_{1\text{-phonon}} > 2$  or  $< 2$ . Compare the potential energy surfaces: Fig.3 in the first item of Ref. [8] and Fig.3 in Ref. [46]; in general, stiff potentials as the former lead to high  $E_{2\text{-phonon}}/E_{1\text{-phonon}}$  ratios while soft ones as the latter do low ratios.

To summarize, two phonon  $\gamma$  vibrational bands in rotating odd- $A$  nuclei were observed recently in three nuclides [26–28]. After these observation, the first theoretical calculation by means of the triaxial projected shell model to one of them was reported [29]. In the present paper, we have applied to the same nuclide a completely different, mean field based model, which was previously developed for the signature dependent properties of one quasiparticle

(zero phonon) bands and later utilized for the  $E2$  intensity relations in one phonon bands. In the present calculation, after confirming almost perfect reproduction of the zero and one phonon states, we concentrated on the effect of the odd quasiparticle on the distribution of the two phonon collectivity. The obtained  $K = \Omega + 4$  state is almost pure at  $\omega_{\text{rot}} = 0$ , but small rotation immediately delivers the strength to two other sequences; consequently three collective sequences keep about 60% collectivity up to higher spins. This indicates future experimental observation of more than one sequence of the  $2\gamma$  bands as well as the other sequence of the  $1\gamma$ . The restriction of the model space mentioned above would be the reason of the result that the calculated  $2\gamma$  states locate higher than observed.

There are some to improve the present calculation: First of all, the model space should be enlarged to more than two phonon states. Further, extension of the microscopic approach by means of the selfconsistent collective coordinate method [8] to rotating even and odd- $A$  systems is promising in future.

### Acknowledgments

The author thanks K. Matsuyanagi and Y. R. Shimizu for valuable comments.

---

- [1] W. F. Davidson et al., J. Phys. **G7** (1981), 455; 843.
- [2] D. D. Warner, R. F. Casten and W. F. Davidson, Phys. Rev. Lett. **45** (1980), 1761; Phys. Rev. **C24** (1981), 1713.
- [3] A. Bohr and B. R. Mottelson, Phys. Scripta **25** (1982), 28.
- [4] A. Bohr and B. R. Mottelson, *Nuclear Structure Vol. II* (Benjamin, New York, 1975).
- [5] T. S. Dumitrescu and I. Hamamoto, Nucl. Phys. **A383** (1982), 205.
- [6] V. G. Soloviev and N. Yu. Shirikova, Z. Phys. **A301** (1981), 263; Yad. Fiz. **36** (1982), 1376 [Sov. J. Nucl. Phys. **36** (1982), 799].
- [7] M. Matsuo, Prog. Theor. Phys. **72** (1984), 666.
- [8] M. Matsuo and K. Matsuyanagi, Prog. Theor. Phys. **74** (1985), 1227; *ibid.* **76** (1986) 93; *ibid.* **78** (1987), 591.
- [9] R. Piepenbring and M. K. Jammar, Nucl. Phys. **A481** (1988), 81.

[10] N. Yoshinaga, Y. Akiyama and A. Arima, Phys. Rev. Lett. **56** (1986), 1116; Phys. Rev. **C38** (1988), 419.

[11] H. G. Börner et al., Phys. Rev. Lett. **66** (1991), 691; 2837.

[12] M. Oshima et al., Phys. Rev. **C52** (1995), 3492.

[13] T. Härtlein, M. Heinebrodt, D. Schwalm and C. Fahlander, Eur. Phys. J. **A2** (1998), 253.

[14] V. G. Soloviev, A. V. Sushkov and N. Yu. Shirikova, Phys. Rev. **C51** (1995), 551.

[15] C. Fahlander et al., Phys. Lett. **B388** (1996), 475.

[16] P. E. Garrett et al., Phys. Rev. Lett. **78** (1997), 4545.

[17] F. Corminboeuf et al., Phys. Rev. **C56** (1997), R1201.

[18] Y. Sun et al., Phys. Rev. **C61** (2000), 064323.

[19] A. S. Davydov and G. F. Filippov, Nucl. Phys. **8** (1958), 237.

[20] W. Korten et al., Phys. Lett. **B317** (1993), 19.

[21] W. Korten et al., Z. Phys. **A351** (1995), 143.

[22] A. Guessous et al., Phys. Rev. Lett. **75** (1995), 2280.

[23] A. Guessous et al., Phys. Rev. **C53** (1996), 1191.

[24] P. G. Bizzeti and A. M. Bizzeti-Sona, Phys. Rev. **C66** (2002), 031301(R).

[25] J. C. Durand and R. Piepenbring, Phys. Rev. **C54** (1996), 189.

[26] H. B. Ding et al., Phys. Rev. **C74** (2006), 054301.

[27] J. -G. Wang et al., Phys. Lett. **B675** (2009), 420.

[28] G. Long et al., Chin. Phys. Lett. **26** (2009), 092502.

[29] J. A. Sheikh, G. H. Bhat, Y. Sun and R. Palit, Phys. Lett. **B688** (2010), 305.

[30] M. Matsuzaki, Y. R. Shimizu and K. Matsuyanagi, Prog. Theor. Phys. **77** (1987), 1302; *ibid.* **79** (1988), 836.

[31] M. Matsuzaki, Nucl. Phys. **A491** (1989), 433; *ibid.* **A519** (1990), 548.

[32] Y. R. Shimizu and T. Nakatsukasa, Nucl. Phys. **A611** (1996), 22.

[33] G. Gervais et al., Nucl. Phys. **A624** (1997), 257.

[34] T. Bengtsson and I. Ragnersson, Nucl. Phys. **A436** (1985), 14.

[35] K. Hara and Y. Sun, Nucl. Phys. **A537** (1992), 77.

[36] Z.-C. Gao, Y. S. Chen and Y. Sun, Phys. Lett. **B634** (2006), 195.

[37] Y. R. Shimizu and K. Matsuyanagi, Prog. Theor. Phys. **67** (1982), 1637; *ibid.* **70** (1983), 144.

[38] V. G. Soloviev, *Theory of Complex Nuclei* (Nauka, Moskow, 1971 [transl. Pergamon Press,

1976]).

- [39] D. de Frenne, Nucl. Data Sheets **110** (2009), 2081.
- [40] Y. Sun et al., Phys. Lett. **B589** (2004), 83.
- [41] D. Janssen and I. N. Mikhailov, Nucl. Phys. **A318** (1979), 390.
- [42] E. R. Marshalek, Nucl. Phys. **A331** (1979), 429.
- [43] S. W. Ødegård et al., Phys. Rev. Lett. **86** (2001), 5866.
- [44] D. R. Jensen et al., Phys. Rev. Lett. **89** (2002), 142503.
- [45] G. Schönwaßer et al., Phys. Lett. **B552** (2003), 9.
- [46] M. Matsuzaki and S. -I. Ohtsubo, Phys. Rev. **C69** (2004), 064317.

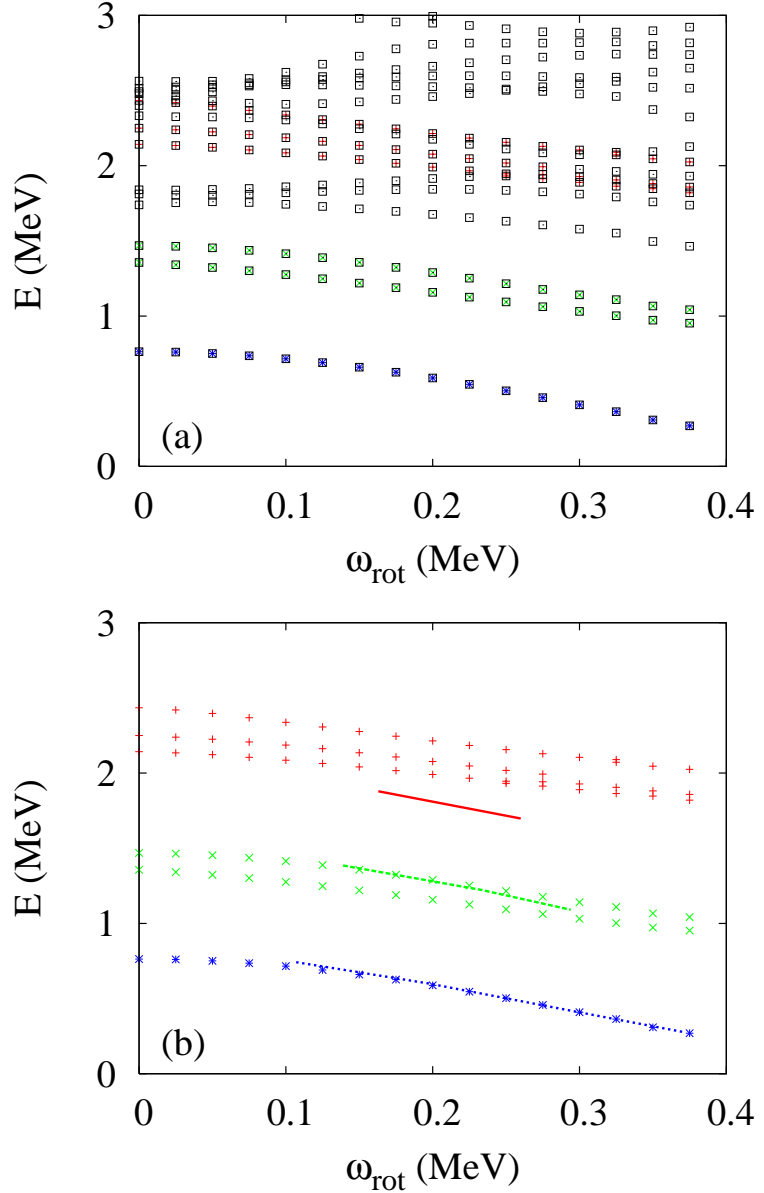


FIG. 3: (Color online) (a) Calculated eigenstates of  $H_{\text{couple}}(\gamma)$  at each rotation frequency. Corresponding to Fig. 2, those with large ( $> 40\%$ )  $\pi[422\,5/2^+] \otimes 0, 1, 2\gamma$  components are marked by symbols. At  $\omega_{\text{rot}} = 0.25, 0.275$  and  $0.325$  MeV, accidental fragmentation caused by interaction with a positive sloping 1qp state occurs. (b) Similar to (a) but the dominantly  $\pi[422\,5/2^+] \otimes 0, 1, 2\gamma$  states are compared with experimental data (curves) converted to the rotating frame by using the Harris parameters  $\mathcal{J}_0 = 15.45 \text{ MeV}^{-1}$  and  $\mathcal{J}_1 = 81.23 \text{ MeV}^{-3}$  that fit the yrast band of  $^{104}\text{Mo}$  [23].